

# Deriving Information Acquisition Criteria For Sequentially Inferring The Expected Value Of A Black-Box Function

Piyush Pandita\*, Ilias Bilonis, Jitesh Panchal

School of Mechanical Engineering, Purdue University, West Lafayette, Indiana 47907

\* ppandit@purdue.edu

## Abstract

*Acquiring information about noisy expensive black-box functions (computer simulations or physical experiments) is a tremendously challenging problem. Finite computational and financial resources restrict the application of traditional methods for design of experiments. The problem is surmounted by hurdles such as numerical errors and stochastic approximations errors, when the quantity of interest (QoI) in a problem depends on an expensive black-box function. Bayesian optimal design of experiments has been reasonably successful in guiding the designer towards the QoI for problems of the above kind. This is usually achieved by sequentially querying the function at designs selected by an infill-sampling criterion compatible with utility theory. However, most current methods are semantically designed to work only on optimizing or inferring the black-box function itself. We aim to construct a heuristic which can unequivocally deal with the above problems irrespective of the QoI. This paper applies the above mentioned heuristic to infer a specific QoI, namely the expectation (expected value) of the function. The Kullback Leibler (KL) divergence is fairly conspicuous among techniques that used to quantify information gain. In this paper, we derive an expression for the expected KL divergence to sequentially infer our QoI. The analytical tractability provided by the Karhunen Loeve expansion around the Gaussian process (GP) representation of the black-box function allows circumvention around numerical issues associated with sample averaging. The proposed methodology can be extended to any QoI, with reasonable assumptions. The proposed method is verified and validated on three synthetic functions with varying levels of complexity and dimensionality. We demonstrate our methodology on a steel wire manufacturing problem.*

**Keywords:** Bayesian experimental design, Kullback Leibler divergence, Design under uncertainty, Gaussian Processes

## 1 Introduction

Numerous engineering problems are represented by either computationally intensive computer codes [47] or expensive physical experiments [15]. With insufficient information about the functional dependence of the objective on the design parameters or experimental conditions, the designer/experimentalist would need hundreds of thousands of experimental data points to establish any sort of belief [26] about the objective. To tackle this problem, design of experiment (DOE) techniques [14, 3, 2] have been investigated and applied on engineering problems. The standard DOE techniques generate a design in a single batch [40], which can be a shortcoming in the case of functions with discontinuities and non-linearity[8]. Also, more useful information gained [11] after a finite number of future experiments can be critical contributors to the *end-goal* of acquiring maximal information about the function.

Techniques for sequential design of experiments have been studied [9, 46] and applied on different applications in experiments [15] and computer simulations [48] for decades.

The sequential design of experiments is also known as *Bayesian optimal design of experiments* (BODE). BODE models the expensive objective function using a cheap surrogate model and selects the design/experiment (from a set of designs) that contains maximal expected value of information. This newly acquired information is included in the surrogate model to update the belief [26] about the objective most commonly using Bayes rule [12]. BODE is usually carried out based on what the designer wants to achieve from the finite number of future experiments/simulations. For example, one could be interested in optimizing the black-box function [35, 27, 17, 25, 34, 16, 39, 22, 4, 23, 32, 37, 30], acquiring information about the objective function [36, 29, 50, 5, 20] or, more recently, acquiring information about the parameters of the black-box function [21, 24]. BODE’s advantages come with it being statistically robust [6] and consistent with information theory [10].

In this paper, we focus on extending and generalizing a BODE heuristic that guides experiments for any quantity of interest (QoI) dependent on the underlying black-box function. For example, a designer might want to gain knowledge about the expectation of the function, gradually learn the dependence of the objective on a specific set of input parameters etc. Much like the majority of the work in BODE, we use Gaussian process (GP) [45] surrogates to *emulate* [43] the expensive black-box function.

A heuristic which is general enough and fairly well established in BODE is the Kullback-Leibler divergence (KLD) [31, 38] (also known as relative entropy). The KLD has been used to quantify information gain [51] about the objective function from a hypothetical experiment (an untried design), in consistency with the earlier work of Lindley[33]. The efficacy of the KLD as a heuristic in information acquisition has been extended and demonstrated on the notorious sensor placement problem under different settings of the parameters [41, 23].

Our primary focus here is to organically extend the use of KLD as an information acquisition function (IAF) for inferring a generic QoI. We make use of the truncated Karhunen-Loeve expansion of a stochastic process[1], around the posterior mean of the surrogate GPs (similar to the approach taken in [7]), to represent the black-box function as a function of the input parameters. We derive the analytical expressions for the expected KLD (EKLD) for a particular QoI, the expectation of the black-box function, and demonstrate how the resulting IAF explores the design space sequentially. Apart from being able to converge after starting from a low-sample regime, the methodology displays an *exploration* and *exploitation* characteristic, a ubiquitous characteristic of IAFs. An ingredient that makes visualization and analysis of convergence smooth is the derivation of expressions for the expected value of our QoI. This quantification of uncertainty, similar to [42], is an addendum of our work in this paper.

The rest of the paper is organized as follows: Sec. 2 describes in detail the methodology used, including GP regression Sec. 2.1 and the EKLD Sec. 2.2. The results obtained for three synthetic test problems have been presented in Sec. 3. The steel wire manufacturing problem is briefly explained and treated with the proposed methodology in Sec. 3.6. We summarize the nuances of the methodology including its weaknesses and pitfalls and also comment on future research directions based on our work in Sec. 4.

## 2 Methodology

Throughout the paper we represent the various elements of our state of knowledge and objective as follows:

1.  $\mathbf{X}_n$  are the  $n$  designs at which the simulation/experiment has been conducted i.e.  
 $\mathbf{X}_n = \{\mathbf{x}_1, \dots, \mathbf{x}_n\}$

2.  $\mathbf{Y}_n$  are the values of the model output at the corresponding  $n$  designs i.e.  $\mathbf{Y}_n = \{y_1, \dots, y_n\}$
3. The state of knowledge at any point in time maybe characterized by the  $n$  observed data points,  $\mathbf{D}_n$  where:  $\mathbf{D}_n = \{\mathbf{X}_n, \mathbf{Y}_n\}$ .
4. A hypothetical untried design is denoted by  $\tilde{\mathbf{x}}$ .
5. A hypothetical observation at  $\tilde{\mathbf{x}}$  is denoted by  $\tilde{y}$ .

In consistency with the above notation we describe the QoI mathematically: Let  $\mathbf{x}$  be a random variable with probability density  $p(\mathbf{x})$  supported on  $\mathcal{X}$ . The black-box function in our problem is defined on the  $\mathcal{L}^2$  space and can be expressed as follows:

$$\mathcal{L}^2(\mathbf{x}) = \{f : \mathcal{X} \rightarrow \mathbb{R} \mid \int f^2(\mathbf{x})p(\mathbf{x})d\mathbf{x} < \infty\} \quad (1)$$

Mathematically, we define a QoI for our purposes as:

$$\mathbf{Q} : \mathcal{L}^2 \rightarrow \mathbb{R} \quad (2)$$

for example,

$$\mathbf{Q}[f] = \int f(\mathbf{x})p(\mathbf{x})d\mathbf{x} \quad (3)$$

which happens to be a bounded linear functional, where  $\mathbf{Q}[\cdot]$  is any operator on our function  $f(\cdot)$ . We define the restricted input space as,  $\mathcal{X} = \times_{k=1}^d [\mathbf{x}_{u,k}, \mathbf{x}_{l,k}]$ . Without loss of generality, the same becomes  $\mathcal{X} = \times_{k=1}^d [0, 1]$  in this paper. We wish to update our beliefs about  $\mathbf{Q}$  at each stage while quantifying the epistemic uncertainty at the same time. We select an experiment based on the plausible gain in information contained in it.

## 2.1 Surrogate modeling

Gaussian process regression is a non-parametric Bayesian regression technique, which has found immense application in surrogate modeling. It not only allows the designer to express prior beliefs about the function but also quantifies epistemic uncertainty about the objective conditioned on the knowledge at a given state. We briefly explain the GP regression technique here. More details can be found in [45].

### 2.1.1 Prior Gaussian process

We model our prior beliefs about the black-box function by using a zero mean prior GP. The covariance kernel is defined by a radial basis function (RBF), also known as squared exponential. More specifically the prior representation of the function is:

$$f \sim \text{GP}(0, k) \quad (4)$$

where,

$$k(\mathbf{x}, \mathbf{x}') = k(\mathbf{x}, \mathbf{x}'; \boldsymbol{\psi}) = s^2 \exp \left\{ -\frac{1}{2} \sum_{j=1}^d \frac{(x_j - x'_j)^2}{\ell_j^2} \right\}, \quad (5)$$

The kernel defined in Eq. (5) allows the designer to incorporate knowledge such as smoothness and magnitude of the objective in the prior belief. The symbol  $\ell_j$  in Eq. (5) is known as the lengthscale of the RBF kernel for the  $j^{\text{th}}$  dimension of the design space.

This is a crucial parameter which quantifies the correlation between the function values at two different designs based on the Euclidean distances in the input space. The  $s^2$  in Eq. (5) is known as the signal strength of the GP and is responsible for incorporating the scale of the black-box function. These parameters are known as hyper-parameters of the kernel and we will denote them by  $\boldsymbol{\psi}$ , i.e.  $\boldsymbol{\psi} = \{s^2, \ell_1, \dots, \ell_d\}$ . A user-defined mean function can always be included without any major modifications in the above definition.

### 2.1.2 Modeling the likelihood

The likelihood is defined as a multivariate Gaussian of the observed values,  $\mathbf{Y}_n$ , at the observed designs  $\mathbf{X}_n$ . The mean vector of this Gaussian distribution is the vector of function values  $\mathbf{f}_n$  at observed designs. The covariance matrix can be computed using the structure defined in Eq. (5). These observations are considered to be contaminated with noise which is assumed to be Gaussian with variance  $\sigma^2$ . This noise variance is assumed to be very low in our case of computer simulation design. We augment the vector of hyper-parameters to include this additional parameter to get  $\boldsymbol{\theta} = \{\boldsymbol{\psi}, \sigma^2\}$ . The joint distribution of the function values at the observed designs is given as follows:

$$p(\mathbf{Y}_n | \mathbf{X}_n, \boldsymbol{\theta}) \sim \mathcal{N}(\mathbf{Y}_n | \mathbf{f}_n, \mathbf{K}_n(\boldsymbol{\psi}) + \sigma^2 \mathbf{I}_n) \quad (6)$$

where,  $\mathbf{K}_n$  is a  $n \times n$  matrix defined according to Eq. (5). It is worth mentioning a crucial step in the machinery at this point. The hyper-parameter values are commonly optimized to *fit* the observed data by maximizing the likelihood probability defined in Eq. (6). Though the ideal way to proceed would be to infer these parameters using a fully Bayesian treatment [18], we aim to deal with it in the future.

### 2.1.3 Posterior distribution

The posterior predictive distribution at a set of untried designs is a GP also, known as the posterior GP. The posterior predictive mean and variance at an untried design can be written in analytical form.

$$p(f(\cdot) | \mathbf{Y}_n, \mathbf{X}_n, \boldsymbol{\theta}) = \text{GP}(f(\cdot) | m_n(\mathbf{x}; \boldsymbol{\theta}), k_n(\mathbf{x}, \mathbf{x}'; \boldsymbol{\theta})) \quad (7)$$

where,

$$m_n(\mathbf{x}; \boldsymbol{\theta}) = (\mathbf{k}_n(\mathbf{x}; \boldsymbol{\psi}))^T (\mathbf{K}_n(\boldsymbol{\psi}) + \sigma^2 \mathbf{I}_n)^{-1} \mathbf{Y}_n, \quad (8)$$

$$\boldsymbol{\alpha} = (\mathbf{K}_n(\boldsymbol{\psi}) + \sigma^2 \mathbf{I}_n)^{-1} \mathbf{Y}_n, \quad (9)$$

and

$$\begin{aligned} k_n(\mathbf{x}, \mathbf{x}'; \boldsymbol{\theta}) &= k(\mathbf{x}, \mathbf{x}'; \boldsymbol{\psi}) \\ &\quad - (\mathbf{k}_n(\mathbf{x}; \boldsymbol{\psi}))^T (\mathbf{K}_n(\boldsymbol{\psi}) + \sigma^2 \mathbf{I}_n)^{-1} \mathbf{k}_n(\mathbf{x}'; \boldsymbol{\psi}) \end{aligned} \quad (10)$$

where  $\mathbf{k}_n(\mathbf{x}; \boldsymbol{\psi}) = (k(\mathbf{x}, \mathbf{x}_1; \boldsymbol{\psi}), \dots, k(\mathbf{x}, \mathbf{x}_n; \boldsymbol{\psi}))^T$ . Specifically for an untried design point  $\mathbf{x}$ , we can derive from Eq. (7) the *point-predictive probability density* for the function conditioned on the hyperparameters  $\boldsymbol{\theta}$ :

$$p(f(\mathbf{x}) | \mathbf{X}_n, \mathbf{Y}_n, \boldsymbol{\theta}) = \mathcal{N}(f(\mathbf{x}) | m_n(\mathbf{x}; \boldsymbol{\theta}), \sigma_n^2(\mathbf{x}; \boldsymbol{\theta})), \quad (11)$$

where  $\sigma_n^2(\mathbf{x}; \boldsymbol{\theta}) = k_n(\mathbf{x}, \mathbf{x}; \boldsymbol{\theta})$ . For concise notation, we choose to write  $m_n(\mathbf{x}; \boldsymbol{\theta})$  as  $m_n(\mathbf{x})$  and the variance at a point  $\sigma_n^2(\mathbf{x}; \boldsymbol{\theta})$  as  $\sigma_n^2(\mathbf{x})$ . This aptly characterizes the state of knowledge about the function after a particular set of observations have been made. In sequential design, this process of updating the GP model and its hyper-parameters takes place each time new data is added. Thus the state of knowledge is augmented with each additional data point.

### 2.1.4 Karhunen Loeve expansion of a GP

A very important ingredient in our proposed methodology is the ability to express the function in a manner that allows us to take samples of the function. Eventually each of these samples of the function would contribute to the  $Q[f(\cdot)]$  we seek to infer.

The Karhunen Loeve expansion (KLE) [19] of the standard Gaussian Process (GP) can be written as follows:

$$f(\mathbf{x}; \boldsymbol{\xi}) = m_n(\mathbf{x}) + \sum_{i=1}^{\infty} \xi_i \sqrt{\lambda_{n,i}} \phi_{n,i}(\mathbf{x}) \quad (12)$$

In Eq. (12) the term  $m_n(\mathbf{x})$  stands for the posterior predictive mean of the function at a design point  $\mathbf{x}$  as derived in Eq. (11). The stochastic variables  $\boldsymbol{\xi}$  are independent standard normal variables Eq. (14). We resort to making use of a truncated expansion of the Eq. (12), which can be written as:

$$f(\mathbf{x}; \boldsymbol{\xi}) \approx m_n(\mathbf{x}) + \sum_{i=1}^W \xi_i \sqrt{\lambda_{n,i}} \phi_{n,i}(\mathbf{x}) \quad (13)$$

where,

$$p(\boldsymbol{\xi}) = \mathcal{N}(0, \mathbf{I}_W) \quad (14)$$

The eigenvalues  $\lambda_{n,i}$ s and corresponding eigenfunctions  $\phi_{n,i}(\mathbf{x})$ s are obtained via the Nystrom approximation. A rigorous tutorial about the step-wise implementation of the same can be found in [7]. The same implementation has been followed in our work. The number of  $\lambda_{n,i}$ s,  $W$ , is determined by the designer by specifying the percentage  $\beta$  of the total mass of the eigenvalues to be retained Eq. (15).

$$\sum_{i=1}^W \lambda_{n,i} = \beta \sum_{i=1}^{\infty} \lambda_{n,i} \quad (15)$$

Consider a possible untried design  $\tilde{\mathbf{x}}$  and its corresponding observation  $\tilde{y}$ . The point distribution of  $\tilde{y}$  conditioned on  $\boldsymbol{\xi}$  is a Gaussian distribution with a variance  $\sigma^2$ .

$$p(\tilde{y}|\tilde{\mathbf{x}}, \boldsymbol{\xi}, \mathbf{D}_n) = \mathcal{N}(m_n(\tilde{\mathbf{x}}) + \sum_{i=1}^w \xi_i \sqrt{\lambda_{n,i}} \phi_{n,i}(\tilde{\mathbf{x}}), \sigma^2) \quad (16)$$

Deriving the posterior of  $\boldsymbol{\xi}$ , or the distribution of  $\boldsymbol{\xi}$  conditional on the  $\mathbf{D}_n$ ,  $\tilde{\mathbf{x}}$  and  $\tilde{y}$ , by completing the squares results in the following:

$$\begin{aligned} p(\boldsymbol{\xi}|\tilde{\mathbf{x}}, \tilde{y}, \mathbf{D}_n) &\propto p(\tilde{y}|\boldsymbol{\xi}, \tilde{\mathbf{x}}, \mathbf{D}_n)p(\boldsymbol{\xi}) \\ &\Rightarrow p(\boldsymbol{\xi}|\tilde{\mathbf{x}}, \tilde{y}, \mathbf{D}_n) = \mathcal{N}(\tilde{\boldsymbol{\mu}}_p, \tilde{\boldsymbol{\Sigma}}_p) \end{aligned} \quad (17)$$

where,

$$\tilde{\boldsymbol{\mu}}_p = \tilde{\boldsymbol{\Sigma}}_p \mathbf{a}^T \left( \frac{\tilde{y} - m_n(\tilde{\mathbf{x}})}{\sigma^2} \right) \quad (18)$$

$$\tilde{\boldsymbol{\Sigma}}_p = \left( \mathbf{I}_W + \mathbf{a}^T \mathbf{a} \frac{1}{\sigma^2} \right)^{-1} \quad (19)$$

where,

$$\mathbf{a} = \left[ \sqrt{\lambda_{n,1}} \phi_{n,1}(\mathbf{x}), \dots, \sqrt{\lambda_{n,W}} \phi_{n,W}(\mathbf{x}) \right] \quad (20)$$

$$\tilde{\Sigma}_p = \mathbf{I}_W - \frac{\mathbf{a}^T \mathbf{a}}{\sigma^2 + \mathbf{a} \mathbf{a}^T} \quad (21)$$

where  $A$  is a row vector as defined in Eq. (20). We obtain Eq. (21) by using the Sherman-Morrison formula [49] on the Eq. (19).

$$\tilde{\Sigma}_{p,ij} = \delta_{ij} - \frac{\sqrt{\lambda_{n,i}} \sqrt{\lambda_{n,j}} \phi_{n,i}(\mathbf{x}) \phi_{n,j}(\mathbf{x})}{\sigma^2 + \sum_{i=1}^W (\sqrt{\lambda_{n,i}} \phi_{n,i}(\mathbf{x}))^2} \quad (22)$$

where  $\delta_{ij}$  is the Kronecker delta. For ease of notation and preferential use of certain expressions in the forthcoming sections we also define the following:

$$\tilde{\boldsymbol{\mu}}_p = \tilde{\boldsymbol{\mu}}_{cp} \left( \frac{\tilde{y} - m_n(\tilde{\mathbf{x}})}{\sigma^2} \right) \quad (23)$$

where,

$$\tilde{\boldsymbol{\mu}}_{cp} = \tilde{\Sigma}_p \mathbf{a}^T \quad (24)$$

## 2.2 Deriving information acquisition function using KL divergence

We aim to demonstrate the functionality of the KL divergence as a metric of information gain towards the QoI from a hypothetical experiment. The KL divergence is a measure that contains the information about how differently the two distributions represent the random variable. In our case, we can interpret the KL divergence between the distribution in Eq. (28) and the one in Eq. (32) as the information gained about the QoI by running the experiment at a particular untried design. Thus, the greater the KL divergence, the greater is the merit in conducting the experiment at the design. This argument constructs the foundation for what we seek to do in later parts of the paper while selecting the design point for the next experiment.

$$\text{KLD}(q_{pos}(\mathbf{Q}) || q_{prior}(\mathbf{Q})) = \int_{-\infty}^{\infty} q_{post}(\mathbf{Q}) \log \frac{q_{post}(\mathbf{Q})}{q_{prior}(\mathbf{Q})} d\mathbf{Q} \quad (25)$$

For a generic QoI,  $\mathbf{Q}$ , we aim have the ability to obtain samples from  $q_{prior}(\mathbf{Q})$  using sample paths of  $p(f(\cdot) | \mathbf{D}_n)$  from Eq. (13) and Eq. (14). Similarly, samples from  $q_{post}(\mathbf{Q})$  can be obtained by using sample paths of  $p(f(\cdot) | \tilde{\mathbf{x}}, \tilde{y}, \mathbf{D}_n)$  from Eq. (13) and Eq. (17). The hypothetical observation is a probabilistic quantity with the distribution defined in Eq. (7). The average value of the KLD over all possible values of the hypothetical observation is the function we look to maximize over the design space. Formally, we represent the task at hand as follows:

$$\mathbf{x}^* = \arg \max_{\mathbf{x}} \int_{-\infty}^{\infty} \int_{-\infty}^{\infty} q_{post}(\mathbf{Q}) \log \frac{q_{post}(\mathbf{Q})}{q_{prior}(\mathbf{Q})} d\mathbf{Q} p(\tilde{y} | \tilde{\mathbf{x}}, \mathbf{D}_n) d\tilde{y} \quad (26)$$

We, approach the above problem for our QoI in this paper, without going into the numerical details of solving Eq. (26) for arbitrary QoIs.

### 2.2.1 Deriving the KL information gain for the expectation of a function

The prior and posterior (with hypothetical observation) that probabilistically characterize our QoI, expectation of a function, can be analytically derived. This proof of concept hinges on the prior Eq. (14) and posterior Eq. (17) distributions of  $\boldsymbol{\xi}$ , both of which are

Gaussian. The QoI here, can be written as:

$$\begin{aligned} \mathcal{Q}[f] &= \int_{\mathbb{R}^d} f(\mathbf{x})p(\mathbf{x})d\mathbf{x} \approx \int_{\mathbb{R}^d} m_n(\mathbf{x})p(\mathbf{x})d\mathbf{x} \\ &\quad + \sum_{i=1}^W \xi_i \sqrt{\lambda_{n,i}} \left( \int_{\mathbb{R}^d} \phi_{n,i}(\mathbf{x})p(\mathbf{x})d\mathbf{x} \right) \end{aligned} \quad (27)$$

We shall denote . Deriving the lower order statistics for the expectation of the function  $f(\mathbf{x}; \boldsymbol{\xi}|D_n)$  presents a closed form expression as shown below:

$$\mathbb{E}[f(\mathbf{x}; \boldsymbol{\xi}|D_n)] \sim \mathcal{N} \left( \int_{\mathbb{R}^d} m_n(\mathbf{x})p(\mathbf{x})d\mathbf{x}, \sum_{i=1}^W \lambda_{n,i} \Psi_{n,i}^2 \right) \quad (28)$$

where  $\Psi_{n,i} = \int_{\mathbb{R}^d} \phi_{n,i}(\mathbf{x})p(\mathbf{x})d\mathbf{x}$ . The mean and variance given in Eq. (28) are obtained by using the standard rule of finding the mean and variance of sum of independent random variables ( $\xi_i$ s, here), where we take  $\mu_1 = \int_{\mathbb{R}^d} m_n(\mathbf{x})p(\mathbf{x})d\mathbf{x}$  and  $\sigma_1^2 = \sum_{i=1}^W \lambda_{n,i} \Psi_{n,i}^2$ . Keeping consistency with above notations in Eq. (2) we can write the same as:

$$p(\mathcal{Q}|\mathbf{D}_n) \sim \mathcal{N}(\mu_1, \sigma_1^2) \quad (29)$$

Expressions for  $\mu_1$  can be derived using the Gaussian tractability of the posterior mean of the GP. We skip the details of that derivation here and simply write the final result below:

$$\int_{\mathbb{R}^d} m_n(\mathbf{x})p(\mathbf{x})d\mathbf{x} = s^2 \sum_{i=1}^n \alpha_i \left( \prod_{k=1}^d \epsilon_k(\mathbf{x}_{i,k}) \right) \quad (30)$$

where,

$$\epsilon_k(\mathbf{x}_{i,k}) = \frac{\sqrt{\pi}}{2} \sqrt{2\ell_k} \left\{ \operatorname{erf} \left( \frac{\mathbf{x}_{u,k} - \mathbf{x}_{i,k}}{\sqrt{2\ell_k}} \right) - \operatorname{erf} \left( \frac{\mathbf{x}_{l,k} - \mathbf{x}_{i,k}}{\sqrt{2\ell_k}} \right) \right\} \quad (31)$$

where erf represents the standard error function and  $\boldsymbol{\alpha}$  has been defined in Eq. (9) and  $\mathbf{x}_{u,k}$  and  $\mathbf{x}_{l,k}$  represent the maximum and minimum of the k-th dimension of the input space  $\mathcal{X}$  respectively. Let us now look at  $\mathcal{Q}_{\mathbf{D}_n, \bar{\mathbf{x}}, \bar{y}}$  which is the distribution of the expectation of the black-box function if a hypothetical observation is made.

$$p(\mathcal{Q}|\mathbf{D}_n, \bar{\mathbf{x}}, \bar{y}) \sim \mathcal{N}(\mu_2, \sigma_2^2) \quad (32)$$

Applying the formula for sum of correlated random variables from Eq. (17) in Eq. (27) we get the expressions for  $\mu_2$  and  $\sigma_2^2$ .

$$\mu_2 = \int_{\mathbb{R}^d} m_n(\mathbf{x})p(\mathbf{x})d\mathbf{x} + \sum_{i=1}^W \sqrt{\lambda_{n,i}} \Psi_{n,i} \tilde{\boldsymbol{\mu}}_{p,i} \quad (33)$$

and

$$\sigma_2^2 = \sum_{ij} \tilde{\Sigma}_{p,ij} \sqrt{\lambda_{n,i}} \sqrt{\lambda_{n,j}} \Psi_{n,i} \Psi_{n,j} \quad (34)$$

using the posterior mean Eq. (18) and posterior covariance Eq. (19) of  $\boldsymbol{\xi}$ . The KL divergence formula for two Gaussian distributions is analytically tractable [13] and shows

up in Eq. (35).

$$\begin{aligned}
\text{KLD}(p(\mathbf{Q}|\mathbf{D}_n, \tilde{\mathbf{x}}, \tilde{y})||p(\mathbf{Q}|\mathbf{D}_n)) &= \log\left(\frac{\sigma_1}{\sigma_2}\right) \\
&+ \frac{\sigma_2^2}{2\sigma_1^2} \\
&+ \frac{(\mu_2 - \mu_1)^2}{2\sigma_1^2} \\
&- \frac{1}{2}
\end{aligned} \tag{35}$$

Since  $\mu_2$  in Eq. (35) is a function of  $\tilde{y}$ , the part of the expression of KL divergence Eq. (35) it needs to be averaged over the values of this hypothetical observation.

$$p(\tilde{y}|\mathbf{D}_n, \tilde{\mathbf{x}}) = \mathcal{N}(m_n(\tilde{\mathbf{x}}), \sigma_n^2(\tilde{\mathbf{x}})) \tag{36}$$

We simply make use of the analytical tractability of the predictive distribution around  $\tilde{y}$  and attempt to intergate it out from Eq. (35). The above precisely means the following:

$$\begin{aligned}
\mathbb{E}[\text{KLD}(p(\mathbf{Q}_{\mathbf{D}_n, \tilde{\mathbf{x}}, \tilde{y}})||p(\mathbf{Q}_{\mathbf{D}_n}))] &= \int_{-\infty}^{\infty} \left( \log\left(\frac{\sigma_1}{\sigma_2}\right) \right. \\
&+ \frac{1}{2} \frac{\sigma_2^2}{\sigma_1^2} \\
&+ \frac{1}{2} \frac{(\mu_1 - \mu_2)^2}{\sigma_1^2} \\
&\left. - \frac{1}{2} \right) \\
&\frac{1}{\sqrt{2\pi}\sigma_n(\tilde{\mathbf{x}})} \exp\left(-\frac{(\tilde{y}-m_n(\tilde{\mathbf{x}}))^2}{2\sigma_n^2(\tilde{\mathbf{x}})}\right) d\tilde{y}
\end{aligned} \tag{37}$$

Close observation of the integrand in Eq. (37), shows that only the third term which contains  $\mu_1$  and  $\mu_2$  depends on the hypothetical simulation. Observing equation Eq. (35) carefully, one can make use of the difference between the means of the distributions in Eq. (28) and Eq. (33) to obtain:

$$\mu_1 - \mu_2 = \sum_{i=1}^W \sqrt{\lambda_{n,i}} \Psi_{n,i} \tilde{\boldsymbol{\mu}}_{p,i} \tag{38}$$

which can be simplified to

$$\mu_1 - \mu_2 = \left( \frac{y - m_n(\tilde{\mathbf{x}})}{\sigma^2} \right) \sum_{i=1}^W \sqrt{\lambda_{n,i}} \Psi_{n,i} \tilde{\boldsymbol{\mu}}_{cp,i} \tag{39}$$

Now we integrate the third term of the integral in Eq. (37) using the expression obtained in Eq. (39). The integration involves a simple change of intergation variable in one step and the rest of the derivation involves matrix multiplication.



The final result shows the following:

$$\int_{-\infty}^{\infty} (\mu_1 - \mu_2)^2 p(\tilde{y}) d\tilde{y} = \frac{\sigma_n^2(\tilde{\mathbf{x}})}{\sigma^4} \sum_{ij} \mathbf{M}_{ij} \quad (40)$$

where,

$$\mathbf{M}_{ij} = \tilde{\boldsymbol{\mu}}_{cp,i} \tilde{\boldsymbol{\mu}}_{cp,j} \Psi_{n,i} \Psi_{n,j} \sqrt{\lambda_{n,i}} \sqrt{\lambda_{n,j}} \quad (41)$$

The final expression for the expected KL divergence (EKLD) for the expectation of a function can be written as follows:

$$\begin{aligned} EKLD(\tilde{\mathbf{x}}) = \mathbb{E}_{\tilde{y}|\tilde{\mathbf{x}},\mathbf{D}_n} [\text{KLD}(p(\mathbf{Q}_{\mathbf{D}_n,\tilde{\mathbf{x}},\tilde{y}}) || p(\mathbf{Q}_{\mathbf{D}_n}))] &= \log\left(\frac{\sigma_1}{\sigma_2}\right) \\ &+ \frac{1}{2} \frac{\sigma_2^2}{\sigma_1^2} \\ &- \frac{1}{2} \\ &+ \frac{1}{2} \frac{\sigma_n^2(\tilde{\mathbf{x}})}{\sigma^4 \sigma_1^2} \sum_{ij} \mathbf{M}_{ij} \end{aligned} \quad (42)$$

Expanding each term on the right hand side in Eq. (42) and writing the expected KL divergence as a function of the hypothetical design  $\tilde{\mathbf{x}}$ , we get:

$$\begin{aligned} EKLD(\tilde{\mathbf{x}}) &= \\ &\frac{1}{2} \log \left( \frac{\sum_{i=1}^W \lambda_{n,i} \Psi_{n,i}^2}{\sum_{i=1}^W \sum_{j=1}^W \sqrt{\lambda_{n,i}} \sqrt{\lambda_{n,j}} \tilde{\boldsymbol{\Sigma}}_{p,ij} \Psi_{n,i} \Psi_{n,j}} \right) \\ &+ \frac{1}{2} \frac{\sum_{i=1}^W \sum_{j=1}^W \sqrt{\lambda_{n,i}} \sqrt{\lambda_{n,j}} \tilde{\boldsymbol{\Sigma}}_{p,ij} \Psi_{n,i} \Psi_{n,j}}{\sum_{i=1}^W \lambda_{n,i} \Psi_{n,i}^2} \\ &+ \frac{\sigma_n^2(\tilde{\mathbf{x}})}{\sum_{i=1}^W \lambda_{n,i} \Psi_{n,i}^2 \sigma^4} \sum_{i=1}^W \sum_{j=1}^W \mathbf{M}_{ij} \\ &- \frac{1}{2} \end{aligned} \quad (43)$$

Now, we collect the expansions of the various terms of the matrices being multiplied

in Eq. (43) from Eq. (41) and Eq. (24).

$$\begin{aligned}
EKLD(\tilde{\mathbf{x}}) &= \frac{1}{2} \log \left( \frac{\sum_{i=1}^W \lambda_{n,i} \Psi_{n,i}^2}{\sum_{i=1}^W \sum_{j=1}^W \sqrt{\lambda_{n,i}} \sqrt{\lambda_{n,j}} \tilde{\Sigma}_{p,ij} \Psi_{n,i} \Psi_{n,j}} \right) \\
&\quad + \frac{1}{2} \frac{\sum_{i=1}^W \sum_{j=1}^W \sqrt{\lambda_{n,i}} \sqrt{\lambda_{n,j}} \tilde{\Sigma}_{p,ij} \Psi_{n,i} \Psi_{n,j}}{\sum_{i=1}^W \lambda_{n,i} \Psi_{n,i}^2} \\
&\quad + \left\{ \frac{\sigma_n^2(\tilde{\mathbf{x}})}{(\sum_{i=1}^W \lambda_{n,i} \Psi_{n,i}^2) \sigma^4} \right. \\
&\quad \left. \left( \sum_{i=1}^W \sum_{j=1}^W \sqrt{\lambda_{n,i}} \sqrt{\lambda_{n,j}} \Psi_{n,i} \Psi_{n,j} \tilde{\boldsymbol{\mu}}_{cp,i} \tilde{\boldsymbol{\mu}}_{cp,j} \right) \right\} - \frac{1}{2}
\end{aligned} \tag{44}$$

where,

$$\begin{aligned}
\tilde{\boldsymbol{\mu}}_{cp,i} &= \sum_j \left( \delta_{ij} - \frac{\sqrt{\lambda_{n,i}} \sqrt{\lambda_{n,j}} \phi_{n,i}(\tilde{\mathbf{x}}) \phi_{n,j}(\tilde{\mathbf{x}})}{\sigma^2 + \sum_{i=1}^W (\sqrt{\lambda_{n,i}} \phi_{n,i}(\tilde{\mathbf{x}}))^2} \right) \\
&\quad \left( \sqrt{\lambda_{n,j}} \phi_{n,j}(\tilde{\mathbf{x}}) \right)
\end{aligned} \tag{45}$$

In this paper, the QoI is the expectation of a function with respect to the uncertainty in the input. We assume that the function is continuous throughout the input domain. The step by step execution of the above described machinery is summarized in algorithm 1. As a stopping rule, the sampling would stop if the ratio of the maximum EKLD obtained in successive iterations falls below a given tolerance value. We take the stopping tolerance value equal to  $10^{-3}$  for our problems.

### 3 Results

We apply the methodology on two one dimensional (1d) mathematical functions (synthetic problems). In all the problems, the domain of the input is the d dimensional hyper-cube i.e.  $[0, 1]^d$ . For the first two synthetic problems the input domain simply becomes  $[0, 1]$  whereas for the third synthetic problem the input domain is  $[0, 1]^6$ . We optimize the IAF over a set of 500 designs by discretizing the input domain for each of the synthetic problems and the wire problem. The number of initial data points is denoted by  $n_i$ . True values of the QoI for each of the synthetic functions are easily available for comparison. For the wire drawing problem, we use an approximation to the QoI by averaging the outputs obtained by running the expensive black-box code at 1000 different designs chosen using Latin-hypercube sampling (LHS).

#### 3.1 Hyper-parameter calibration

We avoid the calibration of the GP model parameters (using MLE) at the beginning of the algorithm in the case of limited initial data points. Instead with a general understanding about the nature of the response surface of a physical process over the unit cube domain, we fix the values of the hyper-parameters. The hyper-parameters of the GP remain fixed until *enough data* has been acquired. This so-called *enough data* criterion is set equal to

---

**Algorithm 1** Bayesian optimal design of experiment with EKLD as the IAF.

---

**Require:** Observed inputs  $\mathbf{X}_n$ , observed outputs  $\mathbf{Y}_n$ , number of candidate points tested for maximum EKLD at each iteration  $n_d$ , maximum number of allowed iterations  $T$ , stopping tolerance  $\gamma$ .

```

1:  $t \leftarrow 0$ .
2: while  $t < T$  do
3:   Construct the truncated Karhunen Loeve expansion to the posterior of the GP,
   Eq. (13).
4:   Generate a set of candidate test points  $\tilde{\mathbf{X}}_{n_d}$ , e.g., via a latin hypercube design
   [38].
5:   Compute EKLD on all of the candidate points  $\tilde{\mathbf{X}}_{n_d}$  using Eq. (44).
6:   Find the candidate point  $\tilde{\mathbf{x}}_j$  that exhibits the maximum EKLD.
7:   if  $t > 0$  then
8:     if  $\frac{EKLD_{n+t}(\tilde{\mathbf{x}}_j)}{EKLD_{prev}} < \gamma$  then
9:       Break.
10:    end if
11:  end if
12:  Evaluate the objective at  $\tilde{\mathbf{x}}_j$  measuring  $\tilde{y}$ .
13:   $\mathbf{X}_{n+t+1} \leftarrow \mathbf{X}_{n+t} \cup \{\tilde{\mathbf{x}}_j\}$ .
14:   $\mathbf{Y}_{n+t+1} \leftarrow \mathbf{Y}_{n+t} \cup \{\tilde{y}\}$ .
15:   $EKLD_{prev} \leftarrow EKLD_{n+t}(\tilde{\mathbf{x}}_j)$ .
16:   $t \leftarrow t + 1$ .
17: end while

```

---

$10 \times d$  for all the problems. The maximization of the likelihood to estimate the hyperparameters is done only after the *enough data* criterion is met. The effect of this delayed *tuning* is visible and has been explained in the results.

### 3.2 Synthetic problem no. 1

The following 1d function is considered as a test case:

$$f(x) = 4(1 - \sin(6x + 8e^{6x-7})) \quad (46)$$

This function is fairly smooth throughout its domain but contains two local minima. The challenge for the methodology in this case lies in being able to explore the function sufficiently and prevent itself from getting trapped inside one of the two *bowl shaped* regions.

Results for the problem in Eq. (46) show that at the end of the final computation, the queries by the IAF have been made at equally spaced designs across the domain. However, the part of exploring the response surface and then exploiting certain sections of the domain takes place interchangeably throughout the whole run of the algorithm. The semantics of the methodology are driven by sampling areas of high probability on the input space and areas of high predictive variance.

In Fig. 1 (a) and (b), the dotted red line represents the true function Eq. (46). The EKLD is shown by the light blue line. The light golden dots are the observed data at any stage and the green diamond is the design with the maximum EKLD selected by the methodology. The posterior mean of the GP of the black-box function is shown using a thick dark blue line. The orange areas around the posterior mean represent the uncertainty (2.5 percentile and 97.5 percentile) around it. For the GP model kernel (squared exponential) the lengthscale is fixed to 0.2, signal strength to 1.0, and the noise variance to  $1e-6$  (low measurement noise in a computer model).

The reduction in variance around the mean after the end of the final iteration of the

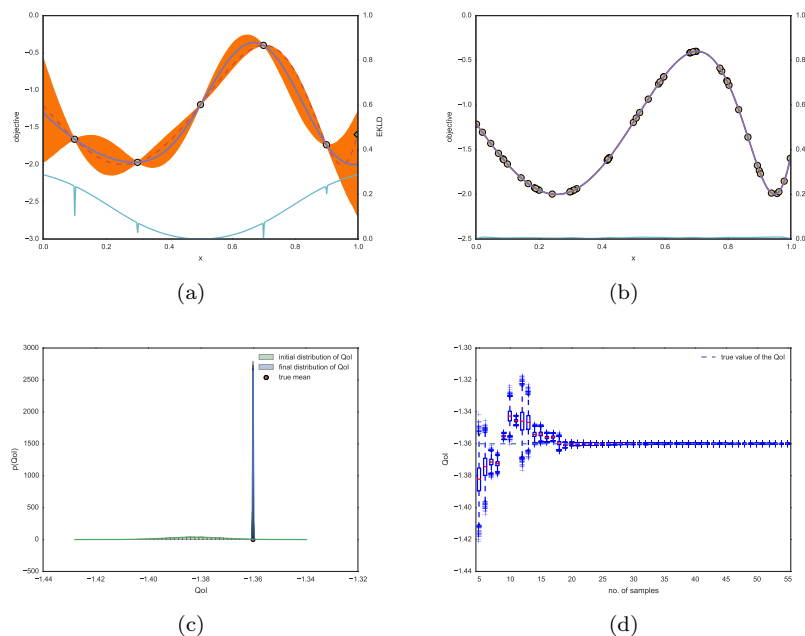


Figure 1: One-dimensional synthetic example ( $n_i = 5$ ). Subfigures (a) and (b) show the state of the function (1st iteration) at the start and the end (50th iteration) of the algorithm. Subfigures (c) and (d) represent the convergence to the true expectation of the function and the reduction in uncertainty about the QoI after the end of the algorithm.

algorithm is shown by Fig. 1 (c). The Fig. 1 (d) shows the estimated mean of  $p(\mathbf{Q}|\mathbf{D}_n)$  and central-limit theorem intervals (2.5 percentile and 97.5 percentile) plotted against the number of data samples. The step-wise reduction in variance in Fig. 1 (d) displays the effect of the delayed tuning mentioned in Sec. 3.1. The methodology reduces the variance even after starting from a low-sample regime until the *enough data* criterion is met (10 for this case). A sudden change in variance can be observed when the number of total samples reaches 10. This is because of the recalibration of the model kernel parameters at this point. The convergence towards the true value of the QoI is shown in Fig. 1 (d).

### 3.3 Synthetic problem no. 2

We consider the following *gaussian mixture* function to test and validate our methodology further.

$$f(x) = \frac{1}{\sqrt{2\pi}s_1} \exp\left(-\frac{(x - m_1)^2}{2s_1^2}\right) + \frac{1}{\sqrt{2\pi}s_2} \exp\left(-\frac{(x - m_2)^2}{2s_2^2}\right) \quad (47)$$

where,  $m_1 = 0.2$  and  $s_1 = 0.05$ ,  $m_2 = 0.8$  and  $s_2 = 0.05$ . As can be seen from Eq. (47), the function is a sum of probability densities of two gaussian distributions. The notoriety of the function lies in two relatively sharp but smaller areas of high magnitude of the function. This could be a challenge especially when the QoI is the expected value of the function. The final state of sampling can be seen in Fig. 2 (b), which shows a fairly equally spaced spread of designs. Intuitively, this is how the methodology is expected to behave when the QoI is the expectation of a function. It is important to note that

Fig. 2 (b) can mislead the reader into perceiving the sampling to be less dense in the areas where the function is sharply peaked. This is an illusion due to the starkly varying ordinates of the sampled points near the peaks of the function. For the GP model kernel (squared exponential) the lengthscale is fixed to 0.05, signal strength to 1.0, and the noise variance to  $1e-6$  (low measurement noise in a computer model) until the *enough data* criterion is met. The convergence of the estimated mean to the true value of the QoI can be seen in Fig. 2 (c) and (d).

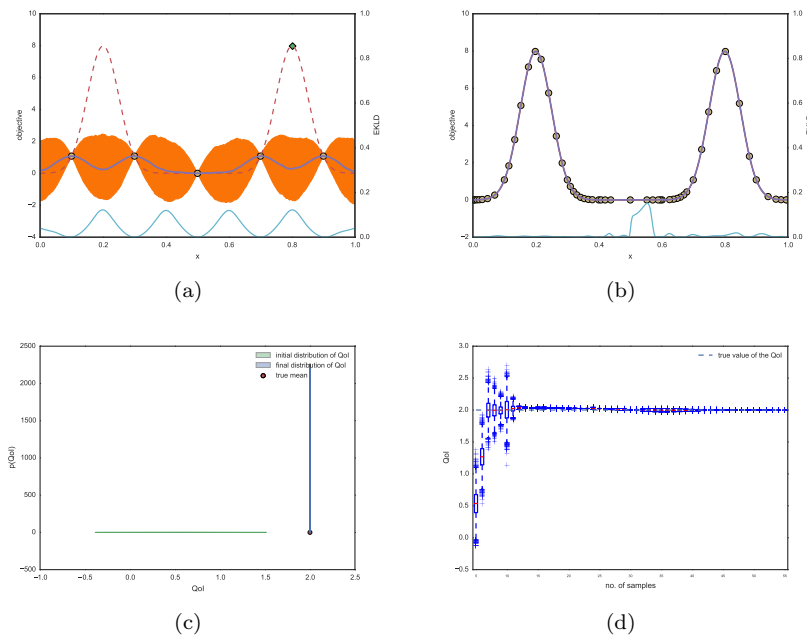


Figure 2: One-dimensional synthetic example ( $n_i = 5$ ). Subfigures (a) and (b) show the state of the function at the start (1st iteration) and the end (50th iteration) of the algorithm. Subfigures (c) and (d) represent the convergence of the function and the reduction in uncertainty about the QoI after the end of the algorithm.

We plot the relative maximum EKLD as a function of the number of samples in Fig. 3 for both the synthetic functions. This relative maximum EKLD is the ratio of the maximum EKLD for the current iteration and the overall maximum EKLD obtained over all the iterations. The plots in Fig. 3 show a characteristic typical of IAFs i.e. of increasing in magnitude for the first few iterations and then falling sharply. This value of the EKLD asymptotically goes to zero for both the synthetic functions here.

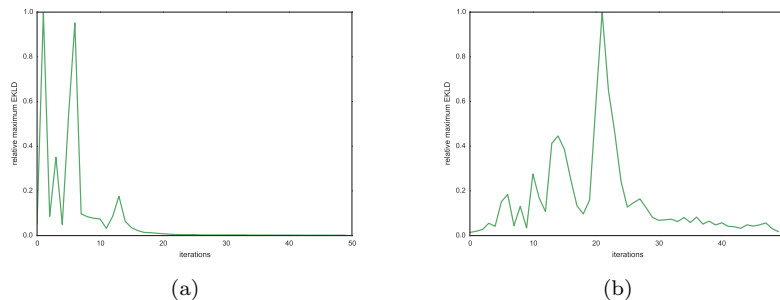


Figure 3: One-dimensional synthetic examples. Subfigures (a) and (b) show the EKLD, for synthetic problem no. 1 ( $n_i = 5$ ) and synthetic problem no. 2 ( $n_i = 5$ ) respectively.

### 3.4 Synthetic problem no. 3

We consider the following six dimensional function from [28] to test and validate our methodology further.

$$f(\mathbf{x}) = \frac{1}{2}(1 - x_1)(1 + g), \quad (48)$$

$$g = 100 \left[ 5 + \sum_{i \in \{2, \dots, 6\}} ((x_i) - 0.5)^2 - \cos(2\pi((x_i) - 0.5)) \right], \quad (49)$$

The major difference between this function Eq. (49) and the ones in the first two synthetic examples is the dimensionality of the problem. The method starts with 40 initial data points, and samples another 80 points. Fig. 4 (a) demonstrates how the relative EKLD tends to approach zero by the end of the sampling process. The iteration-wise approach to the true mean is shown in Fig. 4 (b) and the final distribution of the QoI is shown in Fig. 4 (c). Moreover, the function is used to demonstrate the convergence of the methodology in comparison to uncertainty sampling and random sampling as described in Sec. 3.5.

### 3.5 Comparison to state-of-the art methods

As a demonstration of the performance of the methodology in contrast to two state-of-the-art sampling techniques, namely uncertainty sampling (US) and random sampling (RS) respectively, the method is tested on the synthetic examples given in Sec. 3.2, Sec. 3.3 and Sec. 3.4 respectively. The uncertainty sampling technique works on the principle of reducing the uncertainty around the predictive response surface. The methodology selects a design with the maximum magnitude of predictive variance and follows this procedure until it sequentially acquires the required number of samples. RS selects a design randomly from a pool of designs (generated using LHS) at each iteration of the sampling process. The surrogate modeling process for the US and the RS methodologies works the same way as for the EKLD. The overall algorithm remains the same as 1, but for the change in the sampling criterion.

The convergence to the QoI for the synthetic problem in Sec. 3.2 and Sec. 3.3 is seen in Fig. 5 (a) and Fig. 5 (b) respectively. The US can be seen as being quicker in reaching very close to the true value of the QoI compared to the EKLD and the RS. Overall, the three methodologies converge to the true value in reasonable time of one another and

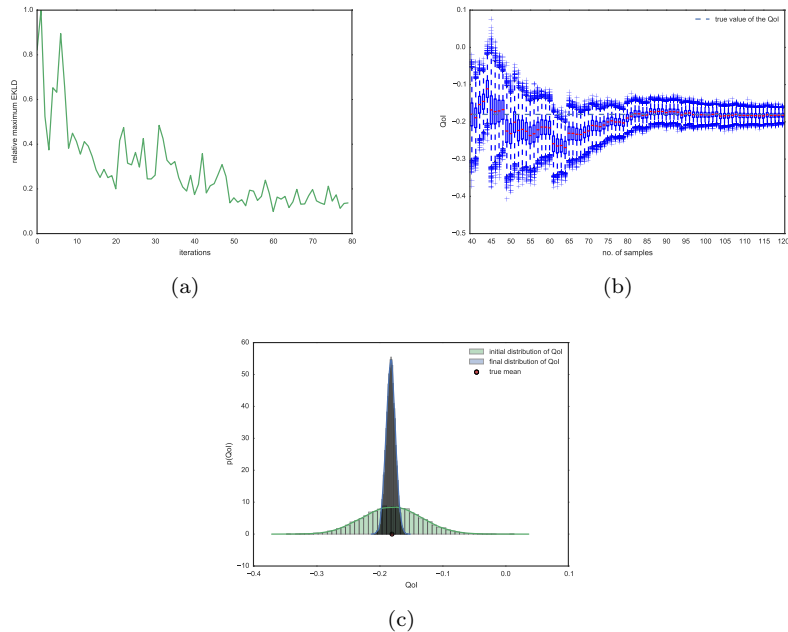


Figure 4: Six-dimensional synthetic example ( $n_i = 40$ ). Subfigure (a) shows the decay of the EKL D from the 1st iteration to the end of the 80th iteration of the algorithm. Subfigures (b) and (c) show the convergence to the true value of the QoI and the final distribution of the QoI after the end of sampling, respectively.

estimate the true mean equally well for the two one-dimensional problems.

However, for the six dimensional synthetic problem, Fig. 5 (c) shows how the EKL D starts to approach the true value of the QoI as the number of iterations increases, whereas the US and the RS tend to show jaggedness in their patterns of convergence. After 80 iterations, the US and the RS patterns seem to show no convergence, but convergence can be seen for the EKL D as early as the addition of the 40th sample. This observation is further strengthened by looking at the decay of the EKL D in Fig. 4 (a). The comparison in Fig. 5 (c) highlights the capability of the methodology to infer the QoI in a limited number of iterations with a high-dimensional function. This is useful in the context of problems with expensive black-box functions where only a few or finite number of more evaluations are possible.

### 3.6 Steel wire drawing problem

The wire drawing process aims to achieve a required reduction in the cross section of the incoming wire, while aiming to monitor or optimize the mechanical properties of the outgoing wire. The incoming wire is passed through a series of dies (8 dies) to achieve an overall reduction in wire diameter. Each pass reduces the cross section of the incoming wire. The authors refer the reader to Section 3.4 in [44] to gain further information about the modeling of the wire drawing process using finite element method. The wire drawing process here is represented by an expensive computer code of which only a finite number of evaluations are possible. The strain non-uniform factor (SNUF) is a mechanical property of the outgoing wire, the expectation of which needs to be inferred, is observed as an output of the expensive computer code. In our problem, we treat the outgoing wire diameter and the die angle as design variables for each pass.

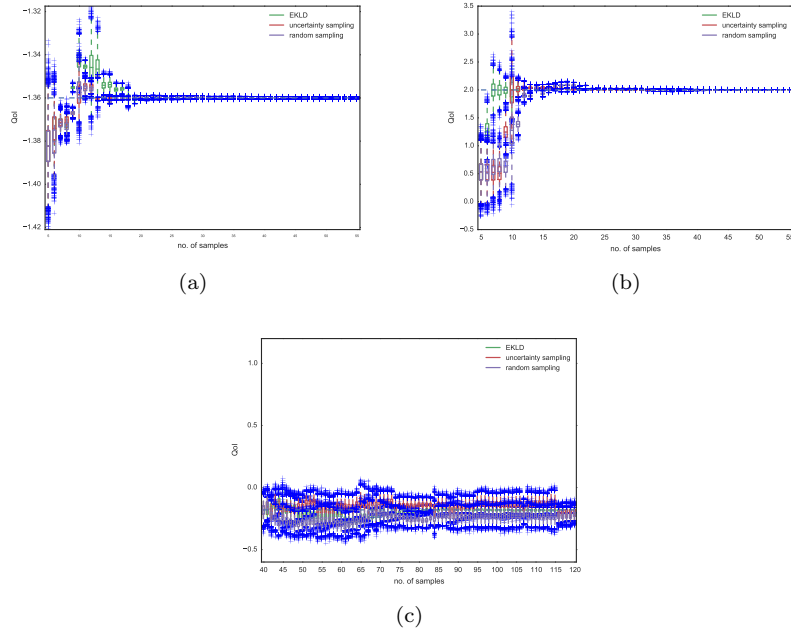


Figure 5: Comparison using synthetic examples. Subfigures (a), (b) and (c) show the convergence to the true value of the QoI, for synthetic problem no. 1 ( $n_i = 5$ ), synthetic problem no. 2 ( $n_i = 5$ ) and synthetic problem no. 3 ( $n_i = 40$ ) respectively.

Since the final outgoing diameter is fixed, the total number of outgoing wire diameters that can vary is seven. Thus, we deal with a total of 15 design variables. We start the problem with 30 initial data points (generated by using LHS), and add another 60 samples sequentially according to the methodology. The results in Fig. 6 show the slow but gradual convergence of the QoI towards the approximated true value. Fig. 6 (a) presents the relative EKL D approaching zero when the sampling is terminated, which is an indication of the very little possible gain in information from further simulations. The reduction in variance around the QoI from the start of the sampling to the end can be seen in Fig. 6 (b). This is intuitive as the number of collected samples increases, the variance around the QoI decreases.

## 4 Conclusions

We presented a methodology for designing experiments to acquire information. The technique relies on the well-established KL divergence to acquire information about the potential gain from a hypothetical design. In this work, the methodology has been used to sequentially conduct simulations to gain information about the expectation of a black-box function. The analytical tractability of the final expressions derived for the expected KL divergence for the QoI investigated in this paper ensures ease and accuracy in computation. The aforementioned characteristic of the methodology for this QoI makes it more robust compared with methods involving sample average approximation. The QoI to be inferred sits inside the mathematical machinery of the methodology and makes the method more flexible to be used across different QoIs. This is in stark contrast with sequential design methods like uncertainty sampling that target gaining more information about only the black-box function. One weakness in the methodology is the fixing of model parameters during the initial phases of sequential design. Unfortunately, the



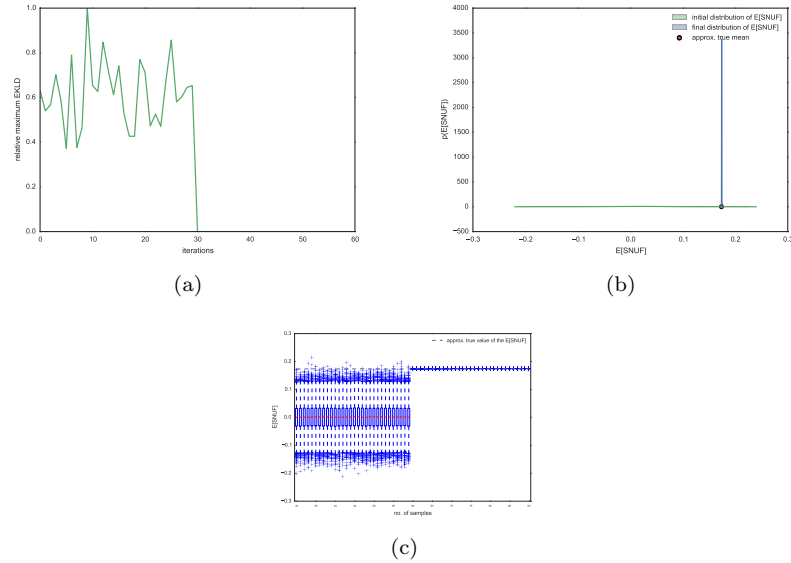


Figure 6: Wire drawing problem ( $n_i = 30$ ) after 60 iterations.

problem of implementing such a generic methodology is not trivial. The most relevant next step to tackle this issue could be to extend the methodology for robust design with non-stationary GPs. In similar vein, the methodology can be well extended to design experiments to infer statistics or quantities of interest which depend on a noisy black-box function. Our future work aims at applying the methodology on more challenging QoIs where analytical tractability is lost.

## 5 Acknowledgments

This work has been made possible by the financial support provided by National Science Foundation through Grant 1662230.

The authors wholeheartedly thank their collaborators at TRDDC, Tata Consultancy Services, Pune, India, for providing the steel wire manufacturing problem.

## References

- [1] A. Alexanderian. A brief note on the karhunen-lo\eve expansion. *arXiv preprint arXiv:1509.07526*, 2015.
- [2] A. Alexanderian, N. Petra, G. Stadler, and O. Ghattas. A-optimal design of experiments for infinite-dimensional bayesian linear inverse problems with regularized  $\ell_0$ -sparsification. *SIAM Journal on Scientific Computing*, 36(5):A2122–A2148, 2014.
- [3] M. J. Anderson and P. J. Whitcomb. *Design of experiments*. Wiley Online Library, 2000.
- [4] P. D. Arendt, D. W. Apley, and W. Chen. Objective-oriented sequential sampling for simulation based robust design considering multiple sources of uncertainty. *Journal of Mechanical Design*, 135(5):051005, 2013.

- [5] J. Beck and S. Guillas. Sequential design with mutual information for computer experiments (mice): emulation of a tsunami model. *SIAM/ASA Journal on Uncertainty Quantification*, 4(1):739–766, 2016.
- [6] J. O. Berger. *Statistical decision theory and Bayesian analysis*. Springer Science & Business Media, 2013.
- [7] I. Bilonis and N. Zabararas. Bayesian uncertainty propagation using gaussian processes. *Handbook of Uncertainty Quantification*, pages 1–45, 2016.
- [8] K. Chaloner and I. Verdinelli. Bayesian experimental design: A review. *Statistical Science*, pages 273–304, 1995.
- [9] H. Chernoff. Sequential design of experiments. *The Annals of Mathematical Statistics*, 30(3):755–770, 1959.
- [10] T. M. Cover and J. A. Thomas. *Elements of information theory*. John Wiley & Sons, 2012.
- [11] B. De Finetti. Bayesianism: its unifying role for both the foundations and applications of statistics. *International Statistical Review/Revue Internationale de Statistique*, pages 117–130, 1974.
- [12] P. Diaconis and S. L. Zabell. Updating subjective probability. *Journal of the American Statistical Association*, 77(380):822–830, 1982.
- [13] J. Duchi. Derivations for linear algebra and optimization. *Berkeley, California*, 2007.
- [14] L. Eriksson, E. Johansson, N. Kettaneh-Wold, C. Wikström, and S. Wold. Design of experiments. *Principles and Applications, Learn ways AB, Stockholm*, 2000.
- [15] N. Flournoy. A clinical experiment in bone marrow transplantation: Estimating a percentage point of a quantal response curve. In *case studies in Bayesian Statistics*, pages 324–336. Springer, 1993.
- [16] P. I. Frazier, W. B. Powell, and S. Dayanik. A knowledge-gradient policy for sequential information collection. *SIAM Journal on Control and Optimization*, 47(5):2410–2439, 2008.
- [17] N. J. Gaul. *Modified Bayesian Kriging for noisy response problems and Bayesian confidence-based reliability-based design optimization*. The University of Iowa, 2014.
- [18] A. Gelman, J. B. Carlin, H. S. Stern, D. B. Dunson, A. Vehtari, and D. B. Rubin. *Bayesian data analysis*, volume 2. CRC press Boca Raton, FL, 2014.
- [19] R. G. Ghanem and P. D. Spanos. Stochastic finite element method: Response statistics. In *Stochastic finite elements: a spectral approach*, pages 101–119. Springer, 1991.
- [20] R. B. Gramacy and H. K. Lee. Adaptive design and analysis of supercomputer experiments. *Technometrics*, 51(2):130–145, 2009.
- [21] C. Guestrin, A. Krause, and A. P. Singh. Near-optimal sensor placements in gaussian processes. In *Proceedings of the 22nd international conference on Machine learning*, pages 265–272. ACM, 2005.
- [22] P. Hennig and C. J. Schuler. Entropy search for information-efficient global optimization. *Journal of Machine Learning Research*, 13(Jun):1809–1837, 2012.

- [23] X. Huan and Y. Marzouk. Gradient-based stochastic optimization methods in bayesian experimental design. *International Journal for Uncertainty Quantification*, 4(6), 2014.
- [24] X. Huan and Y. M. Marzouk. Simulation-based optimal bayesian experimental design for nonlinear systems. *Journal of Computational Physics*, 232(1):288–317, 2013.
- [25] D. Huang, T. T. Allen, W. I. Notz, and N. Zeng. Global optimization of stochastic black-box systems via sequential kriging meta-models. *Journal of global optimization*, 34(3):441–466, 2006.
- [26] E. T. Jaynes. *Probability theory: the logic of science*. Cambridge university press, 2003.
- [27] D. R. Jones, M. Schonlau, and W. J. Welch. Efficient global optimization of expensive black-box functions. *Journal of Global optimization*, 13(4):455–492, 1998.
- [28] J. Knowles. Parego: A hybrid algorithm with on-line landscape approximation for expensive multiobjective optimization problems. *IEEE Transactions on Evolutionary Computation*, 10(1):50–66, 2006.
- [29] A. Krause, A. Singh, and C. Guestrin. Near-optimal sensor placements in gaussian processes: Theory, efficient algorithms and empirical studies. *Journal of Machine Learning Research*, 9(Feb):235–284, 2008.
- [30] J. Kristensen, I. Billionis, and N. Zabarar. Adaptive simulation selection for the discovery of the ground state line of binary alloys with a limited computational budget. In *Recent Progress and Modern Challenges in Applied Mathematics, Modeling and Computational Science*, pages 185–211. Springer, 2017.
- [31] S. Kullback and R. A. Leibler. On information and sufficiency. *The annals of mathematical statistics*, 22(1):79–86, 1951.
- [32] R. Lam, K. Willcox, and D. H. Wolpert. Bayesian optimization with a finite budget: An approximate dynamic programming approach. In *Advances in Neural Information Processing Systems*, pages 883–891, 2016.
- [33] D. V. Lindley. On a measure of the information provided by an experiment. *The Annals of Mathematical Statistics*, pages 986–1005, 1956.
- [34] D. Lizotte. *Practical Bayesian Optization*. Thesis, 2008.
- [35] M. Locatelli. Bayesian algorithms for one-dimensional global optimization. *Journal of Global Optimization*, 10(1):57–76, 1997.
- [36] D. J. MacKay. Information-based objective functions for active data selection. *Neural computation*, 4(4):590–604, 1992.
- [37] A. Marco, P. Hennig, J. Bohg, S. Schaal, and S. Trimpe. Automatic lqr tuning based on gaussian process global optimization. In *Robotics and Automation (ICRA), 2016 IEEE International Conference on*, pages 270–277. IEEE, 2016.
- [38] M. D. McKay, R. J. Beckman, and W. J. Conover. A comparison of three methods for selecting values of input variables in the analysis of output from a computer code. *Technometrics*, 42(1):55–61, 2000.
- [39] J. Mockus. *Bayesian approach to global optimization: theory and applications*, volume 37. Springer Science & Business Media, 2012.

- [40] D. C. Montgomery. *Design and analysis of experiments*. John Wiley & Sons, 2017.
- [41] P. Nath, Z. Hu, and S. Mahadevan. Sensor placement for calibration of spatially varying model parameters. *Journal of Computational Physics*, 343:150–169, 2017.
- [42] J. E. Oakley and A. O’Hagan. Probabilistic sensitivity analysis of complex models: a bayesian approach. *Journal of the Royal Statistical Society: Series B (Statistical Methodology)*, 66(3):751–769, 2004.
- [43] A. O’Hagan. Bayesian analysis of computer code outputs: A tutorial. *Reliability Engineering & System Safety*, 91(10-11):1290–1300, 2006.
- [44] P. Pandita, I. Billionis, J. Panchal, B. Gautham, A. Joshi, and P. Zagade. Stochastic multi-objective optimization on a budget: Application to multi-pass wire drawing with quantified uncertainties. *arXiv preprint arXiv:1706.01665*, 2017.
- [45] C. E. Rasmussen and C. K. I. Williams. *Gaussian processes for machine learning*. Adaptive computation and machine learning. MIT Press, Cambridge, MA, 2006.
- [46] H. Robbins. Some aspects of the sequential design of experiments. In *Herbert Robbins Selected Papers*, pages 169–177. Springer, 1985.
- [47] J. Sacks, W. J. Welch, T. J. Mitchell, and H. P. Wynn. Design and analysis of computer experiments. *Statistical science*, pages 409–423, 1989.
- [48] M. Schonlau. Computer experiments and global optimization. 1997.
- [49] J. Sherman and W. J. Morrison. Adjustment of an inverse matrix corresponding to a change in one element of a given matrix. *The Annals of Mathematical Statistics*, 21(1):124–127, 1950.
- [50] R. Stroh, S. Demeyer, N. Fischer, J. Bect, and E. Vazquez. Sequential design of experiments to estimate a probability of exceeding a threshold in a multi-fidelity stochastic simulator. *arXiv preprint arXiv:1707.08384*, 2017.
- [51] P. Tsilifis, R. G. Ghanem, and P. Hajali. Efficient bayesian experimentation using an expected information gain lower bound. *SIAM/ASA Journal on Uncertainty Quantification*, 5(1):30–62, 2017.